Journal of Nuclear Materials 390–391 (2009) 421–424

Contents lists available at ScienceDirect

Journal of Nuclear Materials

journal homepage: www.elsevier.com/locate/jnucmat

Dependence of SOL widths on plasma current and density in NSTX H-mode plasmas

J.-W. Ahn [a,*], R. Maingi [b], J.A. Boedo [a], V. Soukhanovskii [c,1], The NSTX team

[a] University of California – San Diego, San Diego, CA 92093, USA
[b] Oak Ridge National Laboratory, Oak Ridge, TN 37831, USA
[c] Lawrence Livermore National Laboratory, Livermore, CA 94551, USA

ARTICLE INFO

PACS:
52.55.Fa

ABSTRACT

The dependence of various SOL widths on the line-averaged density ($\bar{n}_e$) and plasma current (I_p) for the quiescent H-mode plasmas with Type-V ELMs in the National Spherical Torus Experiment (NSTX) was investigated. It is found that the heat flux SOL width (λ_q), measured by the IR camera, is virtually insensitive to $\bar{n}_e$ and has a strong negative dependence on I_p. This insensitivity of λ_q to $\bar{n}e$ is consistent with the scaling law from JET H-mode plasmas that shows a very weak dependence on the upstream density. The electron temperature, ion saturation current density, electron density, and electron pressure decay lengths (λ_{Te}, λ_{jsat}, λ_{ne}, and λ_{pe}, respectively) measured by the probe showed that λ_{Te} and λ_{jsat} have strong negative dependence on I_p, whereas λ_{ne} and λ_{pe} revealed only a little or no dependence. The dependence of λ_{Te} on I_p is consistent with the scaling law in the literature, while λ_{ne} and λ_{pe} dependence shows a different trend.

1. Introduction

The lifetime of plasma facing components in the future fusion power plant is critically dependent on the peak heat flux that must be accommodated by the targets for a given power flowing into the Scrape-off Layer (SOL) region, P_{SOL}, which is governed by the radial heat flux width, λ_q. There have been a number of publications on the investigation of λ_q variation as a function of various operational parameters such as plasma current (I_p), plasma density (n_e), P_{SOL}, edge safety factor (q_{95}), and toroidal B-field (B_t). In the large aspect ratio geometry, multi-machine scaling laws on λ_q have been constructed both in L- and H-mode plasmas [1,2], as well as the investigation of λ_{Te}, λ_{ne}, and λ_{pe} [3]. In the spherical tokamak (ST) geometry, an L-mode λ_q scaling using the heat flux profiles from the target Langmuir probe measurement was constructed on MAST [4] and investigations of H-mode λ_q dependence, based on the Infrared (IR) camera measurement, on I_p and P_{SOL} were also carried out in NSTX [5,6].

Heat flux to the divertor target can be calculated using electron temperature and radial particle flux density, by

$$q_\perp = \gamma_s kT_e\Gamma_\perp = \gamma_s kT_e\frac{j_{sat}^+}{e}\sin\xi \quad (1)$$

where γ_s is the sheath heat transmission coefficient, $\Gamma_\perp$ is the particle flux incident on the surface, j_{sat}^+ is the ion saturation current density, and ξ is the angle of incidence between the magnetic field lines and the surface. Relation between j_{sat}^+ and n_e, $j_{sat}^+ \propto \sqrt{T_e}n_e$, indicates that $q_\perp$ is also related to n_e, i.e. $q_\perp \propto T_e^{3/2}n_e$. It is also known the pressure gradient in the edge plasma often comes close to a critical gradient which scales as I_p^2 [11,12]. Therefore, it is important to investigate the dependence of λ_{Te}, λ_{ne}, λ_{jsat}, and λ_{pe} on the operation parameters as well as the λ_q dependence on them in order to more efficiently approach an empirical extrapolation to the future machine. There is little work previously done on this subject, particularly in the ST geometry and H-mode plasmas. In this paper, we report the first result of the five relevant SOL widths, λ_{Te}, λ_{ne}, λ_{jsat}, λ_{pe}, and λ_q, for their dependence on $\bar{n}_e$ and I_p in NSTX H-mode plasmas.

2. Experimental setup

Experiments were performed in the NSTX tokamak [8,9] (R = 0.85 m, a < 0.67 m, R/a > 1.27) in lower single null (LSN) discharges, with toroidal magnetic field, B_T = 0.38–0.55 T, plasma current, I_p = 0.7–1 MA, line-averaged electron density $\bar{n}_e$ = 3.2–6.0 × 10^{13} cm^{-3}, and neutral beam (NBI) power of 1–2 MW. The plasmas had relatively lower elongation, κ = 2.0, and triangularity, δ = 0.45. Simultaneous measurements of the upstream T_e, n_e, and j_{sat} and the target $q_\perp$ profiles were made using the fast reciprocating probe [10] and infra-red (IR) camera [5], respectively, in quiescent H-mode plasmas with Type-V ELMs [13]. The fast reciprocating probe measures upstream plasma parameters

* Corresponding author. Address: Princeton Plasma Physics Laboratory, B-220, P.O. Box 451, Princeton, NJ 08540, USA. Present address: Oak Ridge National Laboratory, Oak Ridge, TN 37831, USA.
E-mail addresses: jahn@pppl.gov (J.-W. Ahn), vlad@pppl.gov (V. Soukhanovskii).
1 Presenting author.

0022-3115/$ - see front matter © 2009 Elsevier B.V. All rights reserved.
doi:10.1016/j.jnucmat.2009.01.110

(17.3 cm below the mid-plane) across the SOL with spatial resolution of 1–2 mm. The IR camera measures heat flux profile both on the inboard and outboard divertor tiles with temporal resolution of ~33 ms and spatial resolution of ~6 mm.

Fig. 1 shows the time evolution of (a) plasma current, (b) line averaged density, (c) injected NBI power (P_{NBI}), and (d) D_α signal for outer lower divertor, for a typical Type-V ELM H-mode shot, 128341. The L-H transition is indicated by the D_α drop at ~130 ms, and the plasma stays in H-mode until ~430 ms. The small oscillations on D_α signal are signatures of the Type-V ELMs. The reciprocating probe was plunged during the time window indicated by the dotted vertical lines. The measured profiles by the probe and IR camera are flux mapped to the midplane using the magnetic equilibrium reconstruction and are plotted as a function of $R - R_{sep}$ (radial distance from the separatrix location).

3. Dependence of various SOL widths on I_p and $\overline{n}_e$

The electron–electron collisionality ($\nu^*_{ee} = L_c/\lambda_{ee}$, where λ_{ee} is the e–e mean free path and L_c is the parallel connection length) in the upstream SOL region was calculated from the T_e and n_e profile data and L_c calculated by magnetic equilibrium reconstruction. It is found that the SOL plasma is strongly collisional near the separatrix, (ν^*_{ee} = 30–40, and stays in the conduction-limited regime within a few centimeters from the separatrix [7]. It is found that the SOL plasma profiles are well peaked and decay exponentially within 2–3 cm from the separatrix (the near SOL), and have long tails from there to the wall (the far SOL). Therefore only the near SOL plasma was fitted to the exponential function to obtain scale lengths.

3.1. I_p dependence

The I_p scan was conducted for two I_p levels, 0.8 and 1.0 MA, with approximately constant q_{95} by varying B_t accordingly, with P_{NBI} = 1.4 MW and $\overline{n}_e = 3.5 \times 10^{13}$ cm^{-3} during the measurement. The peak heat flux increased strongly with increasing I_p, while λ_q decreased by a factor of ~2. This is consistent with the previous NSTX result [5,6]. First shown in Fig. 2 is the two ion saturation current profiles measured by the fast probe I_{sat} tip, which is constantly biased to −170 V to obtain particle flux profile. λ_{jsat} has a strong negative dependence on I_p, i.e. 1.1 cm for 1 MA and 1.6 cm for 800 kA. The second plot of Fig. 2 shows two electron pressure profiles, $p_e = T_e n_e$, with T_e and n_e measured by the single probe tip. It is seen that λ_{pe} is virtually independent of the I_p variation. The dependence of λ_{Te} and λ_{ne} on I_p is shown in Fig. 3. Note that for all these profiles the separatrix position determined by the equilibrium reconstruction was corrected by the power balance consideration which gives T_e at the separatrix ($T_{e,sep}$) of 30–40 eV for the shots presented in Figs. 2 and 3. On the other hand, the separatrix position of the IR heat flux profiles is well defined by the position of peak heat flux. It is seen that λ_{Te} has a strong negative dependence on I_p, i.e. λ_{Te} increased by more than 30%, from 1.6 to 2.1 cm, with the I_p decrease from 1 MA to 800 kA. This result is consistent with the H-mode λ_{Te} scaling result from ASDEX-Upgrade (AUG) [3].

$$\lambda_{Te} \propto \overline{n}_e^{0.92\pm0.18} I_p^{-1.79\pm0.27} (P_{tot} - P_{rad})^{-0.63\pm0.09} \quad (2)$$

λ_{Te} in NSTX, ranging usually from ~1.0 to ~2 cm, is much longer than values from conventional tokamaks with comparable size. A recent multi-machine λ_{Te} scaling with major radius, $\lambda_{Te} = 3.1\times 10^{-3} R_0(m)$ [14], would give a much shorter λ_{Te} for NSTX (R_0=0.85 m) than is observed. Same is expected for the plot in λ_{Te}/R_0 vs. $n_{e,sep}/n_{Greenwald}$ space [14]. NSTX results would be a factor of 6–7 higher than the fitting lines in both cases. We suspect this indicates that the minor radius (a) might be a better choice for the machine size scaling than the major radius, considering the different aspect ratio between ST and conventional tokamaks. However, this would not completely resolve the discrepancy, e.g. DIII-D has a similar minor radius with NSTX but λ_{Te} is still 2–3 times

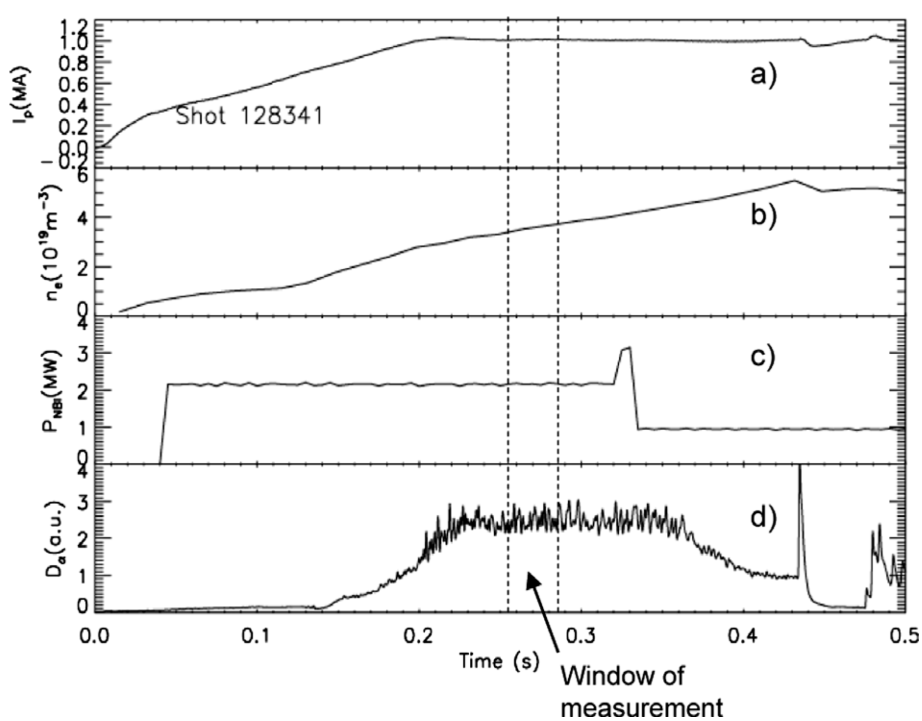

Fig. 1. Time trace of various discharge parameters: (a) plasma current, (b) line-averaged density, (c) injected NBI power, and (d) D_α signal for outer lower divertor. Data was taken during the quiescent H-mode phase with Type-V ELMs. The window indicated by dotted vertical lines is the time period of reciprocating probe measurement.

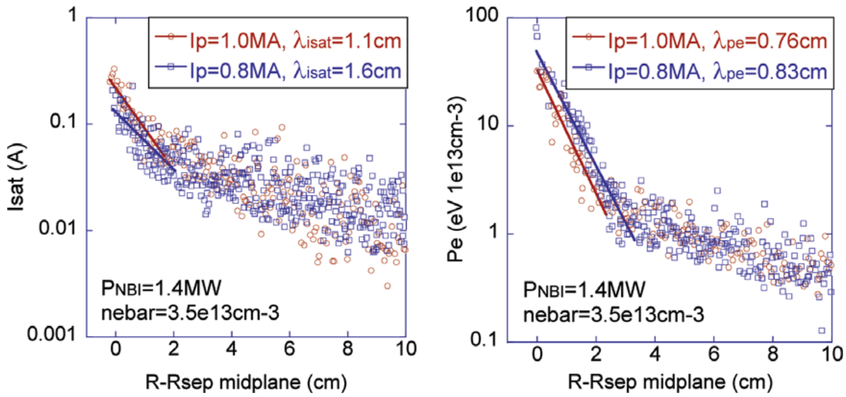

Fig. 2. Measured j_{sat}^{+} (by fast reciprocating probe at $z = -17.3$ cm) profile and p_e (calculated from the measured T_e and n_e profiles, i.e. $p_e = T_e n_e$) profile, mapped to the midplane with fitting curves for the near SOL overlaid, as a function of $R - R_{sep}$ in two I_p cases.

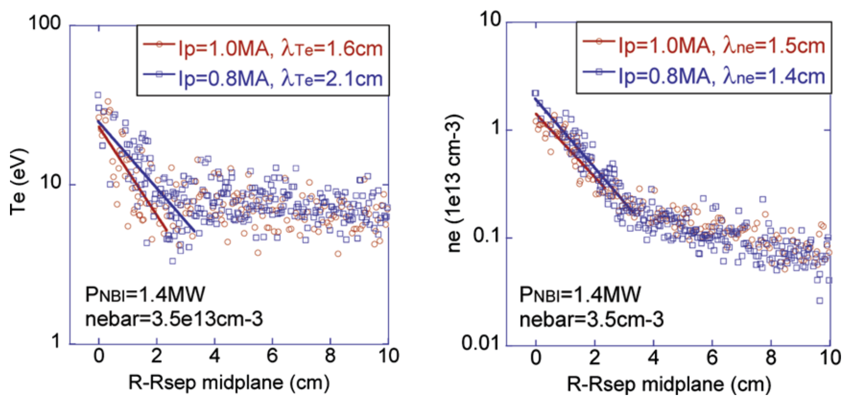

Fig. 3. Measured T_e and n_e profiles (by fast reciprocating probe at $z = -17.3$ cm), mapped to the midplane with fitting curves for the near SOL overlaid, as a function of $R - R_{sep}$, for the same discharges as in Fig 2.

smaller than NSTX. One possibility that could explain this is the effect of ELM filaments on broadening T_e profile, which is a topic of our on-going investigation.

On the other hand, little change in λ_{ne} is observed. It slightly increased, from 1.4 cm to 1.5 cm, with the I_p increase from 800 kA to 1 MA. However, this change could be within the error bar associated with the probe measurement and certainly the dependence of λ_{ne} on I_p is much weaker than λ_{Te} and λ_{jsat}. This result is not consistent with the H-mode λ_{ne} scaling result from AUG [3]

$$\lambda_{ne} \propto \overline{n}_e^{1.11\pm0.13} I_p^{-2.25\pm0.16} \tag{3}$$

from which a significant λ_{ne} decrease (~40%) is expected with the I_p increase from 800 kA to 1 MA. This insensitivity of λ_{ne} to I_p is the primary cause of the invariance of λ_{pe} against the I_p variation (Fig. 2). This result is also in contrast to a λ_{pe} scaling law in the literature [3,11]

$$\lambda_{pe} \propto \overline{n}_e^{1.03\pm0.13} I_p^{-1.96\pm0.2} (P_{tot} - P_{rad})^{-0.4\pm0.07} \tag{4}$$

λ_{pe} scaling as $\lambda_{pe} \propto \overline{n}_e / I_p^2$, with heat diffusivities scaling similarly [15], is largely consistent with the expectation from critical gradient limitation by pressure driven modes (e.g. ideal or resistive ballooning modes) [11,12]. This suggests that NSTX edge plasma might not totally consistent with the ballooning-mode-type profile characteristics. However, considering the small size of our present database and therefore the limited parameter range and large error bars, it seems inappropriate to make a definite conclusion at this stage.

Also, by plotting Thomson scattering T_e and n_e data against each other, a clear correlation between radial electron density and temperature decay lengths is found, with $\eta_e = d(\ln T_e)/d(\ln n_e)$ ranging from 1.2 to 1.9, in the steep pedestal gradient region inside and across the separatrix for Type-V ELMy and ELM-free H-mode plasmas. This could be consistent with a critical η_e behavior typical for drift modes [12]. One interesting point observed in NSTX is that η_e often has a break point in the near SOL, slightly past the separatrix toward the wall, from where data points toward the core show $\eta_e = 1.2$–1.9 and data points toward the wall has a weaker functional form, $\eta_e = 0.4$–0.8.

3.2. $\overline{n}_e$ dependence

The λ_q dependence on $\overline{n}_e$ in L-mode plasmas is found stronger in the ST geometry ($\lambda_q \propto \overline{n}_e^{1.5}$) [4] than in the conventional tokamaks ($\lambda_q \propto \overline{n}_e^{0.68}$) [1]. On the other hand, the multi-machine H-mode λ_q scaling in the conventional tokamak geometry [1] does not contain dependence on $\overline{n}_e$. A more recent result from JET ELMy H-mode plasmas [2] indicates that λ_q dependence on the upstream density is weakly positive. That is,

$$\lambda_q \propto B_t^{-0.9} q_{95}^{0.4} P_{SOL}^{-0.5} n_{e,u}^{0.15} \tag{5}$$

Our investigation of λ_q dependence on $\overline{n}_e$ in H-mode plasmas is based on a dataset with density variation of about ~50% (from 4.0 to 6.0×10^{13} cm^{-3}). It is seen that λ_q stays almost the same over the whole range of density variation, at around $\lambda_q = 1.2$–1.5 cm. The result shown in Fig. 4 is for a discharge with $I_p = 900$ kA and $P_{NBI} = 2$ MW. The JET result (Eq. (5)), based on a multi-shot dataset, would anticipate virtually same λ_q values over the density variation of 50% because of its weak density dependence. Therefore, it appears consistent with our result. This scaling law does not have

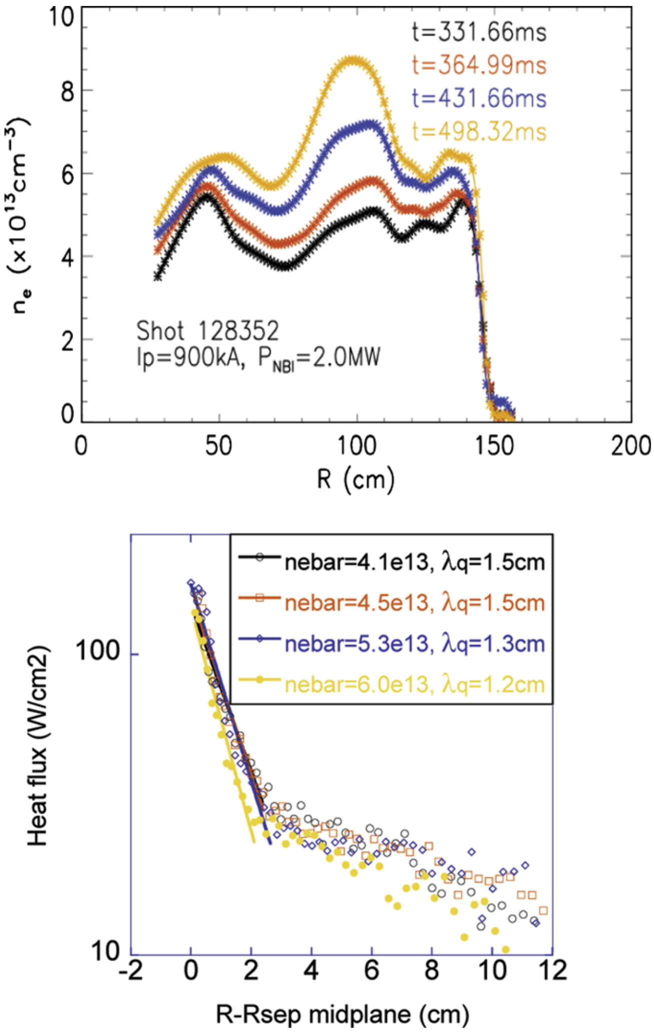

Fig. 4. Measured heat flux profiles at the outer lower divertor tile by IR camera with near SOL fitting curves overlaid (lower) and n_e profile by Thomson Scattering (upper) in four line-averaged density cases, corresponding to different time slices during a long H-mode period for shot 128352.

an I_p dependence but the B_t dependence can be interpreted as the I_p dependence as we have kept q_{95} constant during the I_p scan experiment ($I_p \propto q_{95}B_t$). Therefore, the negative dependence of λ_q on I_p in NSTX mentioned earlier is also consistent with Eq. (5). The negative dependence of λ_q on the input power, which was reported previously [5,6], shows the same trend as is expected from Eq. (5) as well. The λ_{Te}, λ_{jsat}, λ_{ne}, and λ_{pe} dependence on $\overline{n}_e$ could not be investigated due to the lack of measured data points and is a subject for further study in the future.

4. Discussions

The negative dependence of λ_q on I_p confirms our previous result [5,6] and the result of no dependence on $\overline{n}_e$ is consistent with the JET result [2]. The strong negative dependence of λ_{Te} on I_p is consistent with the scaling law from AUG database [3]. However, our result of no dependence of λ_{ne} on I_p shows a different trend from the scaling law in the literature. The λ_{Te} and λ_{ne} dependence on $\overline{n}_e$ will be also investigated and compared with the existing scaling laws in the future. Collisionality and connection length for NSTX are not obviously different from the ones in conventional tokamaks. Typical NSTX values are $\nu_e^* \sim 30$ and $L_c = 40–50$ m near the separatrix. Although the connection length is longer than conventional tokamaks with comparable minor radius (e.g. $L_c \leqslant 30$ for both ASDEX-U and DIII-D), SOL collisionality values are similar ($\nu_e^* = 15–45$ for both machines [3]). We therefore do not expect that the longer connection length would make a big difference in the scaling result by itself. As for the relevant size parameter for multi-machine comparison, we believe the minor radius would be a better choice because of the low aspect ratio of NSTX, as was discussed earlier.

Considering the limited size of our present database, there is a need for a bigger dataset to further investigate dependences on I_p and $\overline{n}_e$ as well as to derive scaling laws and extrapolation to the future machine. Data analysis to construct a larger dataset for T_e and n_e profiles is currently underway. It is suspected that the observed insensitivity of λ_{ne} to I_p, therefore insensitivity of λ_{pe} as well, might be related to the different confinement properties and this will be investigated in detail in the future work.

Acknowledgement

This work was supported by the US Department of Energy, contract numbers DE-FG02-03ER54731, DE-AC02-76CH03073, DE-AC05-00OR22725, and DE-AC52-07NA27344.

References

[1] A. Loarte et al., J. Nucl. Mater. 266–269 (1999) 587.
[2] W. Fundamenski, S. Sipila, Nucl. Fus. 44 (2004) 20.
[3] K. McCormick et al., J. Nucl. Mater. 266–269 (1999) 99.
[4] J-W. Ahn, G.F. Counsell, A. Kirk, Plasma Phys. Control. Fus. 48 (2006) 1077.
[5] R. Maingi et al., J. Nucl. Mater. 363–365 (2007) 196.
[6] R. Maingi et al., in: Proc. of 34th EPS Conf., Warsaw, Poland, 2007.
[7] J-W. Ahn, J.A. Boedo, R. Maingi, V. Soukhanovskii, Phys. Plasmas 15 (2008) 122507.
[8] M. Ono et al., Nucl. Fus. 40 (2000) 557.
[9] S.M. Kaye et al., Nucl. Fus. 45 (2005) S168.
[10] J.A. Boedo et al., Rev. Sci. Instrum., submitted for publication.
[11] B. Labombard et al., Phys. Plasmas 15 (2008) 056106.
[12] J. Neuhauser et al., Plasma Phys. Control. Fus. 44 (2002) 855.
[13] R. Maingi et al., Phys. Plasmas 13 (2006) 092510.
[14] A. Kallenbach et al., J. Nucl. Mater. 337–339 (2005) 381.
[15] J.W. Kim et al., J. Nucl. Mater. 290–293 (2001) 644.